3D electromagnetic simulation of spatial autoresonance acceleration of electron beams

V D Dugar-Zhabon[1], J D González[2] and E A Orozco[1]

[1] Universidad Industrial de Santander, Bucaramanga, Colombia.
[2] Universidad del Magdalena, Santa Marta, Colombia.

E-mail: jedgonzalezac@unal.edu.co

Abstract. The results of full electromagnetic simulations of the electron beam acceleration by a TE_{112} linear polarized electromagnetic field through Space Autoresonance Acceleration mechanism are presented. In the simulations, both the self-sustaned electric field and self-sustained magnetic field produced by the beam electrons are included into the elaborated 3D Particle in Cell code. In this system, the space profile of the magnetostatic field maintains the electron beams in the acceleration regime along their trajectories. The beam current density evolution is calculated applying the charge conservation method. The full magnetic field in the superparticle positions is found by employing the trilinear interpolation of the mesh node data. The relativistic Newton-Lorentz equation presented in the centered finite difference form is solved using the Boris algorithm that provides visualization of the beam electrons pathway and energy evolution. A comparison between the data obtained from the full electromagnetic simulations and the results derived from the motion equation depicted in an electrostatic approximation is carried out. It is found that the self-sustained magnetic field is a factor which improves the resonance phase conditions and reduces the beam energy spread.

1. Introduction

The self-sustenance of the cyclotron resonance interaction between the electron and the transverse electromagnetic wave propagated along a homogeneous magnetic field, has been known since 1962 as cyclotron autoresonance [1, 2] which can be realized in various ways [3]. An autoresonance accomplished in a homogeneous magnetic field which increases in time to compensate precisely a relativistic deflection of the electron cyclotron movement phase on the wave phase is known as GYRAC [4]. A cyclotron autoresonance acceleration of electrons in a guide inhomogeneous magnetostatic field by a travelling electromagnetic wave is analyzed in [5,6]. Electron acceleration to high energies by microwaves in inhomogeneous magnetostatic field found in the numerical experiments on plasma dynamics in an Electron Cyclotron Resonance (ECR) minimum-B trap [7] is attributed to a self-sustenance of the ECR conditions on some parts of the electron trajectory. An acceleration of protons by a circularly polarized electromagnetic wave propagates along a homogeneous guided field is studied in [8]. The results of self-sustenance of the ECR conditions in the static inhomogeneous magnetic field at a fixed microwave field frequency both through a numerical simulation and an analytical analysis were reported in [9–11]. This acceleration mode was named Spatial Autoresonance Acceleration (SARA). In the SARA concept, the determined magnetostatic field profile along the electron beam trajectory makes possible a compensation of the electron mass relativistic change by the corresponding variation

of the magnetic field magnitude [10]. In such a manner the equality between the microwave frequency and the electron cyclotron frequency is maintained during the beam motion. An electrostatic (PIC) code [11] is used to analyze the influence of the self-consistent electric field on the space autoresonance interaction. For an X ray source certificated recently [12], the attainable electron energy has been calculated in the simulations based on this concept. To appreciate the significance of the magnetic field generated by electron beam, the SARA numerical simulations are fulfilled using a full electromagnetic (EM) PIC code, and the obtained results are compared with those calculated in the electrostatic approximation. In this code, the finite difference time domain (FDTD) method is put to use [13]. The beam current density is calculated by using the charge conservation method [14]. The relativistic Newton-Lorentz equation presented in the centered difference form is solved applying the Boris algorithm that provides visualization of the beam path and its energy, velocity and phase evolutions [15].

2. Theoretical formalism

The physical scheme of the autoresonant accelerator is shown in Figure 1. A magnetron (4) emits 2.45GHz microwaves into TE_{112} cylindrical cavity (1) through a waveguide (3), a ferrite isolator (5) and an iris window (6). To avoid non-physical reflections of the microwaves in the waveguide, we apply the Uniaxial Perfectly Matched Layer (UPML) method [16]. The perfectly matched layer is located before the TE_{10} excitation plane in the rectangular waveguide. The microwaves fill the cavity through a rectangular iris window of $7.65 \times 1.0cm^2$. The length and radius of the cylindrical cavity are $4.54cm$ and $20cm$, respectively. To attain the microwave steady-state regime in the cavity as soon as possible, the Hanning function is applied [17] on the assumption that the cavity and waveguide walls are made of the perfect electric conductor material. Once the microwave field achieves the steady state regime of amplitude of $E_0^l = 14kV/cm$, the cold electron beam of $1.0A$ or $3.0A$ is injected into the cavity through an orifice of $0.2cm$ in radius along the magnetic field axis which is taken as z-axis. The initial longitudinal energy of the beam electrons is $14keV$.

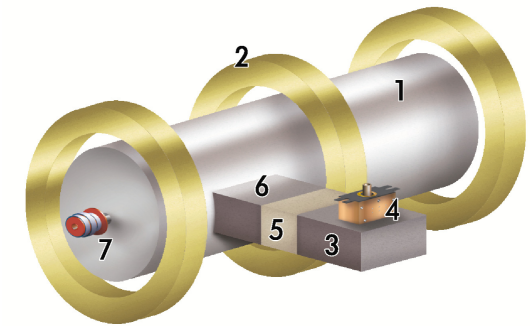

Figure 1. Physical scheme of the autoresonant system: 1-cavity, 2-magnetic coils system, 3-waveguide, 4-magnetrón, 5-ferrite isolator, 6-window, 7-electron gun.

The SARA space configuration of the axially symmetric magnetostatic field is formed by a system of three DC current coils (2). All the parameters referring to the coil currents are identical to those described in [11].

The beam motion is depicted in the framework of the Vlasov-Maxwell equation system:

$$\frac{\partial f_e}{\partial t} + \vec{v} \cdot \frac{\partial f_e}{\partial \vec{r}} - e(\vec{E} + \vec{v} \times \vec{B}) \cdot \frac{\partial f_e}{\partial \vec{p}} = 0 \tag{1}$$

$$\vec{\nabla} \times \vec{E} = -\frac{\partial \vec{B}}{\partial t}, \qquad \vec{\nabla} \times \vec{B} = \mu_0 \vec{J} - \varepsilon_0 \frac{\partial \vec{E}}{\partial t} \tag{2}$$

where f_e is the electron distribution function and $\vec{E}$ and $\vec{B}$ are the electric and magnetic fields inside the cavity, respectively. The electric field $\vec{E}$ presents the superposition of TE_{112} electric component with the electric field generated by the beam electrons. The magnetic field $\vec{B}$ is composed of the TE_{112} magnetic component, the magnetic field generated by the beam electrons and the magnetostatic field produced by the coil system. The superparticle charge density and current density are determined by the expressions:

$$\rho(\vec{r},t) = -e\int f_e d\vec{p}, \quad \text{and} \quad \vec{J}(\vec{r},t) = -e\int \vec{v} f_e d\vec{p} \tag{3}$$

The equations system (1)-(3) is solved through using a (PIC) method [15]. The single superparticle (SP) dynamics is described with the following motion equations:

$$\frac{d\vec{r}_k}{dt} = \vec{v}_k, \qquad \frac{d(\gamma m_k \vec{v}_k)}{dt} = q_k(\vec{E}_P + \vec{v_k} \times \vec{B}_P) \tag{4}$$

where $\gamma = [1-(v_k/c)^2]^{-1/2}$ is the relativistic factor, $q_k(=-N_e e)$ and $m_k(=N_e m_e)$ are the charge and mass of a SP, $\vec{E}_p$ and $\vec{B}_p$ are the total electric and magnetic fields at the position of the k-th SP, respectively. The SP positions and velocities are found using the Boris leapfrog procedure [15]. In the electrostatic approximation (ES) the electric self-consistent field is determined in the mesh nodes by solving the Poisson equation at each time step, and a trilinear interpolation helps determine this field in the SP positions [11]. In order to obbtain the beam trajectory and its energy under the electromagnetic approach (EM), the Newton-Lorentz equation and the Maxwell equations are calculated jointly. The Maxwell equations in the finite difference form are:

$$\vec{B}^{n+1/2} = \vec{B}^{n-1/2} - \vec{\nabla} \times \vec{E}^n \tag{5}$$

$$\vec{E}^{n+1} = \vec{E}^n + \frac{\Delta t}{\varepsilon_0}[\mu_0 \vec{J}^{n+1/2} - \vec{\nabla} \times \vec{B}^{n+1/2}] \tag{6}$$

Where n is the index of the time step ($t_n = n \triangle t$). The self-consistent magnetic and electric fields are calculated on the mesh points using the Yee technique [13]. The fields $\vec{E}_p$ and $\vec{B}_p$ in the SP localization points are found with the help also a trilinear interpolation method. Starting from the initial data on the positions and velocities of the *SPs*, the current density is computed applying the charge conservative method [14]. In the simulations all the quantities are taken in dimensionless form: $\vec{E}^* = \vec{E}/(-B_0 c)$, $\vec{B}^* = \vec{B}/(-B_0)$, $\vec{J}^* = \mu_0 \vec{J}/(r_{l0} B_0)$, $\vec{r}^* = \vec{r}/r_{l0}$ and $t^* = \omega t$; where: $B_0 = m_e \omega / e$ is the magnetic induction corresponding to the classic cyclotron resonance for the electrons and $r_{l0} = c/\omega$ is the relativistic Larmor radius. The phase difference between the particle velocity vector and the right-hand electric field component of the microwave field is calculated indirectly. The simultaneous numerical solution of the motion equations (4) and Maxwell equations (5), (6) permits to calculate the electron positions, particle energy and longitudinal velocity at any time step.

3. Results and discussion

The simulations are fulfilled on a rectangular mesh with the following spatial steps: $\Delta x = \Delta y = 0.07cm$, $\Delta z = 0.2cm$ at a time step $\Delta t = 2.07ps$ chosen in accordance with the Courant stability condition [16]. Each superparticle consists of 3×10^5 electrons.

For the superparticles, the simulation is considered completed when it hits the lateral cavity wall or reaches a plane where the longitudinal velocity goes to zero which is due to the diamagnetic force. Figure 2 shows the image of the distribution of the microwave electric field component in the cross section $z = L_c/4$.

Figure 3 shows a snapshot of the electron beam trajectory in the SARA conditions. One can see that the Larmor radius of the electron whose guiding center which moves along the magnetic field axis grows smoothly because the energy of the electrons associated with the transversal motion is increased.

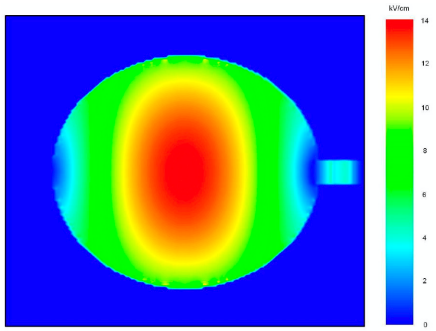

Figure 2. Microwave electric field component in the cross section $z = L_c/4$ before injection of electron beam.

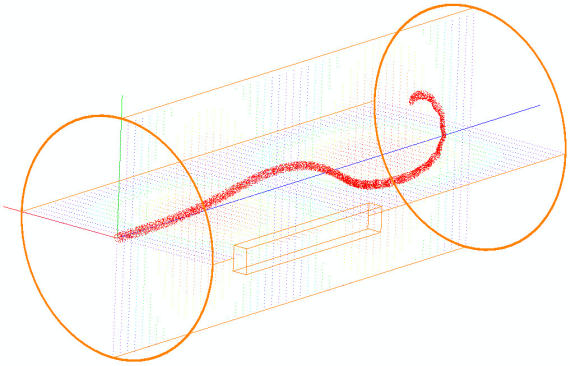

Figure 3. Snapshot of the electron beam in SARA conditions.

In Figure 4 (a) for $1A$ beam, the phase difference φ between the transverse electron velocity and the right-hand polarized microwave electric component after 9.72 microwave periods calculated for the ES and EM approaches is presented.

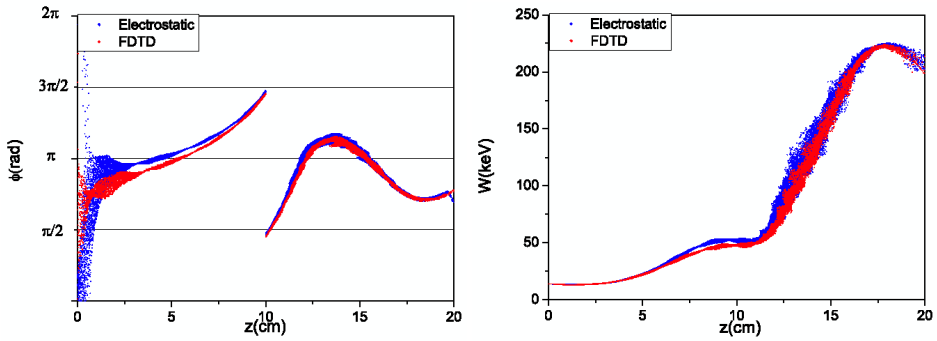

(a) (b)

Figure 4. (a) Phase shift between the electric field of the right hand component of the microwaves field and the transversal velocities of electrons for $1A$ beam after 9.72 microwave cycles. Red dots correspond to FDTD simulations and blue dots to ES simulations. (b) Energy of a $1A$ beam after 9.72 microwave cycles.

The simulations show that in the EM case the beam occupies a smaller phase space in comparison with the case of the ES approximation. A direct consequence of this effect is a decrease of the energy spread along the beam trajectory, as compared with the ES (see Figure

4(b)). Since the only difference between these two approaches is the self-consistent magnetic field, we can conclude that the proper beam magnetic field opposes to the radial beam electric field and the diffusion of electrons in the phase space. It is important to note that the self-consistent magnetic field considerably diminishes the initial beam phase range as compared with the ES results and promotes the electron phase focalization. In the case of $1A$ beam, the focalization occurs at a distance of $1cm$ from the injection orifice where the electrons come into the exact autoresonance acceleration regime. The beam motion beyond the focalization point is found auto-maintained in the acceleration phase range $(\pi/2, 3\pi/2)$. The phase jump at $z = 10cm$ shown in Figure 4 (a) is due to the fact that this point is a TE_{112} microwave field node. Figure 4 indicates that the self-consistent magnetic field does not affect the maximum energy value, which means that its magnitude is insufficient to change the resonance conditions. This circumstance manifests itself through the practical equality of the longitudinal β_z and the transversal β_T electron velocity data obtained for the ES and EM simulations (see Figure 5).

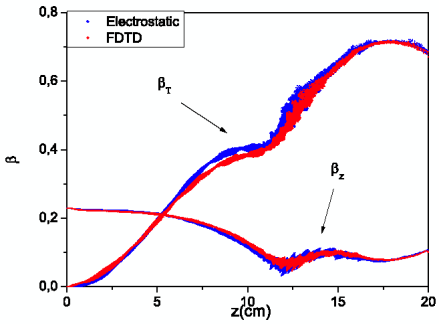

Figure 5. Transversal β_T and longitudinal β_Z components for $1A$ beam after 9.72 microwave cycles. Red dots correspond to FDTD simulations and blue dots to ES simulations.

A more significant influence of the self-consistent electric field on the beam characteristics is observed for the $3A$ beam. Figure 6(a) shows that the phase focalization length of $3.5cm$ is larger than in $1A$ case. This length increase can be attributed to a higher self-consistent electric field which opposes the focalization effect. For this reason, the energy spread of the $3A$ beam is found considerably larger in comparison with $1A$ case (see Figures 5 and 6(b)). It should be noted that the radial self-consistent electric field and longitudinal magnetostatic field provoke a motion of electrons around the beam center. This motion also results in longitudinal velocity decrease. The electron density in the neighborhood of $z = 10cm$ point increases due to decelerating of the diamagnetic force at diminishing of the microwave field (see Figure 7).

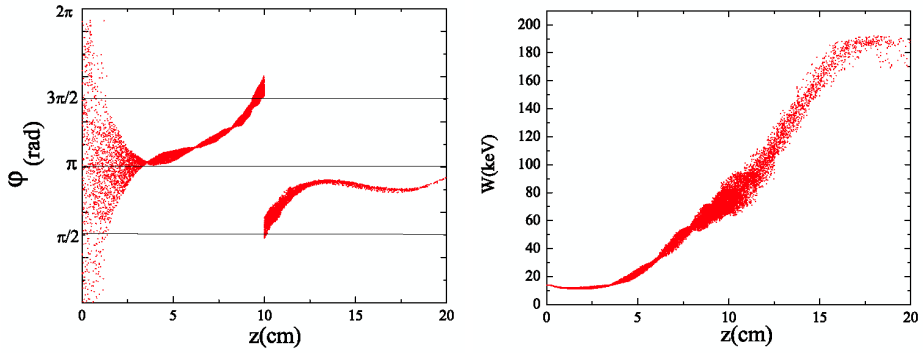

(a) (b)

Figure 6. (a) Phase shift between the microwaves and the transversal velocities of electrons for $3A$ beam after 8 microwave cycles. (b) Beam electron energy for $3A$ beam.

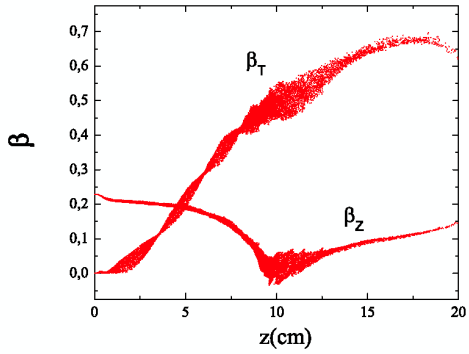

Figure 7. Transversal β_T and longitudinal β_Z components for $3A$ beam after 8 microwave cycles.

4. Conclusions

The executed space autoresonance 3D numerical simulations using an electromagnetic particle in cell code show that the studied system based on a TE_{112} cylindrical cavity can accelerate electron beams of $1A$ and $3A$ to energies of hundreds kilo-electron-volts. The different behaviour of $1A$ beam and $3A$ beam injected into the chamber through the same orifice is explained by the discrepancy in their densities which results in a difference in the self-consistent electric fields. It is shown that the self-consistent magnetic field reduces the beam phase area and energy spread. A further step to go into the system efficiency under study, namely the microwave power harnessing and variation of the microwave frequency is scheduled.

Acknowledgments

This work is supported by Foundation for Promotion for Research and Technology (Bank of Republic) under contract No 201123, Magdalena University (Fonciencias) and the Colombian Agency COLCIENCIAS through doctoral scholarships 567.

References

[1] A Kolomenskii and A Levedev 1962 *Dokl Akad Nauk USSR* **145** 1251
[2] V Davydovskii 1962 *Zh Eksp Teor Fiz* **43** 886
[3] V Milantiev 2013 *Physics Uspekhi* **56** 823
[4] K S Golovanivsky 1983 *IEEE Trans PLasma Sci* **11** 28
[5] R Shpitalnik, C Cohen, F Dothan and L Friendland 1991 *J Appl Phys* **70** 1101
[6] L Friendland 1994 *Phys Plasmas* **1** 421
[7] V Dougar-Jabon, A Umnov and D Suescún 2002 *Rev Sci Instrum* **73** 629
[8] A Holkundkar, G Brodin and M Marklund 2012 *Phys Rev ST-AB* **15** 091301
[9] V Dugar-Zhabon, E A Orozco and A Umnov 2008 *Phys Rev ST-AB* **11** 041302
[10] V Dugar-Zhabon and E A Orozco 2009 *Phys Rev ST-AB* **12** 041301
[11] V Dugar-Zhabon and E A Orozco 2010 *IEEE Transaction on Plasma Science* **38** 2980
[12] V Dugar-Zhabon and E A Orozco 2011 *Fuente compacta autoresonante de rayos X* (Colombia: Patent 11-112696)
[13] K Yee 1966 *IEEE Trans Ant Propagat* **14** 302
[14] T Umeda 2003 *Comp Phys Com* **156** 73
[15] R W Hockney and W Eastwood 1988 *Computer simulation using particles* (Bristol: A Higler)
[16] A Taflove and S Hagness 2000 *Computational electrodinamics the finite-difference time-domain 2d* (Norwood: M A Artech House)
[17] D Prescott and N Shuley 1994 *IEEE Trans on Micr Theor and Tech* **42** 1582